ISSN 1001-0742
Journal of Environmental Sciences Vol. 18, No. 5, pp. 903—909, 2006 CN 11-2629/X

Article ID: 1001-0742(2006)05-0903-07 CLC number: X131.1; O657.3 Document code: A

Characterization of products from photooxidation of toluene

HAO Li-qing[1], WANG Zhen-ya[1], FANG Li[1], ZHANG Wei-jun[1,*], WANG Wei[2], LI Cheng-xiang[2], SHENG Liu-si[2]

(1. Laboratory of Environmental Spectroscopy, Anhui Institute of Optics and Fine Mechanics, Chinese Academy of Sciences, Hefei 230031, China. E-mail: hlqing@aiofm.ac.cn; 2. National Synchrotron Radiation Laboratory, University of Science and Technology of China, Hefei 230026, China)

Abstract: Photooxidation reaction of toluene in smog chamber systems was initiated by the UV radiation of toluene/CH_3ONO/NOx mixtures. The products of the photooxidation reaction of toluene and its subsequent reactions were analyzed directly utilizing Fourier transform infrared spectrometer (FTIR). Detailed assignments to FTIR spectrum of gas-phase products were given. The information of some important functional groups in the products, such as, carbonyl groups (C=O), hydroxyl groups (—OH), carboxylic acid (—COOH), C=C bonding, N—O bonding and C—H bonding (C—H), was got from this analysis. These results were compared to those analyzed by aerosol time of flight mass spectrometer (ATOFMS). It was found that there are some differences between FTIR analysis of gas-phase products and that of particle-phase, for example, the products with carbonyl groups, which were connected to unsaturated chemical bonds, was relatively higher in the gas phase, while ketones, aldehydes, carboxylic acid and organonitrates were the dominant functional groups in the aerosol-phase reaction products. The possible reaction pathways of some important products in the gas phase were also discussed.

Keywords: toluene; photooxidation; secondary organic aerosol; Fourier transform infrared spectrometer; smog chamber

Introduction

Volatile aromatic compounds are particularly important constituents and comprise up to 44% of the volatile hydrocarbon mixture in the urban atmosphere. Among these aromatics, benzene, toluene, ethylbenzene, xylenes and 1,2,4-trimethylbenzene make up 60%—75% of this load, with toluene being one of the most significant compounds (Jang *et al.*, 2001). Secondary organic aerosol (SOA) could be formed through a process of OH radical-initiated photooxidation reaction (Jang *et al.*, 2001; Odum *et al.*, 1997a; Forstner *et al.*, 1997), acid catalyzed reaction on the surface of particle (Jacob, 2000; Jang *et al.*, 2002) and partitioning of volatile compounds between the gas and particle phase (Odum *et al.*, 1996; Bowman *et al.*, 1997). SOA may have possible impacts on the visibility of air, formation of clouds and human health (Odum *et al.*, 1997b; Kalberer *et al.*, 2004).

The chemical composition of SOA generated in the photooxidation of aromatic hydrocarbon compounds can be analyzed by gas chromatograph/mass spectrometer (GC/MS) (Odum *et al.*, 1997a; Forstner *et al.*, 1997), gas chromatograph/ion trap mass spectrometer (GC/ITMS) (Jang *et al.*, 2001) and chemical ionization gas chromatography ion trap mass spectroscopy (CIGC-ITMS) (Kleindienst *et al.*, 2004). Recently, some theoretical research on the formation of SOA has been done by us (Wang *et al.*, 2005); And we used the aerodynamic particle sizer spectrometer to study the effects of various environmental factors on the formation of SOA from the toluene photooxidation reaction (Hao *et al.*, 2005); a home-made aerosol time of flight mass spectrometer was also employed to detect the chemical composition of SOA from toluene photooxidation reaction (Odum *et al.*, 1997b; Wang *et al.*, 2006).

However, there are some disadvantages in the detection methods mentioned above: GC/MS system can only identify a small fraction of the organic aerosol mass, and the sample preparation may lead to possible secondary chemical reactions or loss of semivolatile compounds associated with traditional aerosol sampling onto a filter of impactor plate, or multi-step chemical treatments; The CIGC-ITMS systems demand strict detection conditions (Frazey *et al.*, 1999); Compared to these detection methods, Fourier transform infrared (FTIR) spectroscopy is capable of characterizing a larger fraction of the sample mass, yielding the information of functional groups for the compounds. Furthermore, measurements can be made directly from particle samples without extraction or other sample processing, and analyses are nondestructive. Using the method of FTIR, laboratory studies have been conducted such as the measurements of gas-phase aromatic compound absorption cross section (Etzkorn *et al.*, 1999), the atmospheric chemistry of benzene (Klotz *et al.*, 1997), the OH-initiated photooxidation reaction of benzene (Volkamer *et al.*, 2002; Klotz *et al.*, 2002), the analysis of aerosol formed in the photooxidation of naphthalene (Dekermenjian *et al.*, 1999a), sesquiterpenes (Dekermenjian *et al.*, 1999b) and toluene (Jang *et al.*, 2001). When FTIR is used to analyze aerosol products, the aerosol is collected on ungreased

Foundation item: The National Natural Science Foundation of China (No. 20477043), the Knowledge Innovation Foundation of Chinese Academy of Sciences (No. KJCX2-SW-H08) and the National Synchrotron Graduation Innovation Foundation of Ministry of Education of China (Hefei);
*Corresponding author

ZnSe discs. Once the aerosol samples are collected, they are analyzed. However, the FTIR spectroscopy used for the direct detection of toluene photooxidation products in the gas phase has not ever reported.

This paper reported the study on the photooxidation of toluene in a home-made smog chamber. The photooxidation products generated in this chamber was directly introduced into the FTIR spectroscopy to obtain the function group information.

1 Experiment

1.1 Materials

Toluene (>99%) was obtained from Sigma-Aldrich Chemistry Corporation, Germany and nitrogen oxide (99.9%) from Nanjing Special Gas Factory. Methyl nitrite was synthesized by the dropping sulfuric acid into a methanol solution of sodium nitrate. Their reaction products passed through saturated sodium hydroxide trap to remove the traces of sulfuric acid, and were dried by passing through a calcium sulfate trap, and collected using a condenser of liquid nitrogen at 77 K. The methyl nitrite was purified using a vacuum system of glass.

1.2 Experimental methods

Photooxidation of toluene was performed using UV-irradiation of toluene/CH_3ONO/NO/air mixtures in our home-made smog chamber, the overall experimental system has been presented in detail (Hao *et al.*, 2005; Wang *et al.*, 2006). The smog chamber was made of quartz tube and its volume was 23.3 L. The reactor was surrounded by 16 fluorescent black lamps used to initiate the photochemical reaction. The output power of each blacklamp is 20 W and its wavelength of UV radiation is in the range of 300—400 nm. Prior to start the experiment, the chamber was continuously flushed with purified laboratory compressed air for 20 min. The compressed air was processed through three consecutive packed-bed scrubbers containing, in order, activated charcoal, silica gel and a Balston DFU (r) filter (Grade BX) respectively, to remove the trace of hydrocarbon compounds, moisture and particles. Toluene was injected directly into the chamber. NO and methyl nitrate were expanded into the evacuated manifold to the desired pressure through Teflon lines, and introduced into the smog chamber by a steam of purified air. The whole system was completely shrouded from sunlight with a black polyethylene tarpaulin. Hydroxyl radicals were generated by the photolysis of methyl nitrite in air at wavelengths longer than 300 nm (Atkinson *et al.*, 1981). The chemical reactions leading to the formation of the OH· radical are

$$CH_3ONO+h\upsilon(>300\ nm) \rightarrow \cdot CH_3O\cdot+NO \quad (1)$$

$$CH_3O\cdot+O_2 \rightarrow \cdot HCHO+HO_2\cdot \quad (2)$$

$$HO_2\cdot+NO \rightarrow \cdot OH\cdot+NO_2 \quad (3)$$

1.3 Products characterization

Photooxidation reaction of toluene in the smog chamber can lead to the generation of gas-and particle-phase compounds. The gas-phase products were analyzed by FTIR to obtain the function group information: firstly, at the start of the experiment, the long-path absorption cell was evaluated to 20 mTorr by a mechanical pump, followed by flushing with purified nitrogen for several times. Then the cell was installed into the Fourier transformation infrared spectrometer (Bomen DA8 Model). The background infrared spectra were recorded for subtraction of background in future. Secondly, a mixture of toluene/CH_3ONO/NO/air was introduced into the smog chamber. The initial concentration of toluene, CH_3ONO and NO was 98.2, 7092 and 2149 ppm, respectively. Once the reactants were thoroughly mixed, they were introduced into the long-path absorption cell until the pressure reached 0.5×10^5 Pa. Record the infrared spectra again. This spectrum presented the absorption of the reactants before they were irradiated. Finally, in the smog chamber, a mixture of 98.2 ppm toluene, 7092 ppm CH_3ONO and 2149 ppm NO was exposed to two black lamps radiation for one hour. The photooxidation of toluene was initiated by hydroxyl radical(·OH) resulting in the formation of secondary organic aerosol. And then, the products was introduced to the absorption cell from the chamber until the pressure of the cell reached 0.5×10^5 Pa again. And then the infrared spectrum is recorded and assigned carefully. Here it should be pointed out that the products in the absorption cell were comprised of both the gas-phase and aerosol-phase compounds, and we mainly obtained the information of gas-phase products in a transmission detection mode of FTIR. In this mode, we can ignore the information in the aerosol-phase products. The spectrometer was equipped with a KBr beam splitter for probing the products in the 4000—800 cm^{-1} range, and a liquid nitrogen cooled HgCdTe detector during the measurement. The scan number and resolution for FTIR were 32 and 2 cm^{-1}, respectively.

The particle-phase products were characterized by ATOFMS to obtain the chemical composition. A detailed detection method has been presented previously (Wang *et al.*, 2006) and will not be described here.

2 Results and discussion

2.1 Gas-phase products analysis

In the past 10 years, some theoretical studies were conducted to predict the composition of products from the OH-initiated toluene photooxidation reaction (Forstner *et al.*, 1997; Uc *et al.*, 2000; Sun *et al.*, 2002; Stroud *et al.*, 2004). Experimental studies were

also done to identify the oxidation products in gas and particle phase of toluene by using different detection methods (Jang and Kamens, 2001; Forstner *et al.*, 1997; Kleindienst *et al.*, 2004; Stroud *et al.*, 2004). Now, the identification of infrared spectrum from toluene-oxidation products will be illustrated on the basis of the references (Jang and Kamens, 2001; Dekermenjian *et al.*, 1999a, b; Wang, 1984). Fig.1 shows the infrared spectrum of ambient air. The wide absorption bands over the range of 3501—3947 cm^{-1} and 1888—1321 cm^{-1} are due to vibration of residual water in the air. The strongest absorption peak at 2362 cm^{-1} is due to C—O asymmetrical stretching vibration of CO_2. Besides these, no other absorption peaks are found.

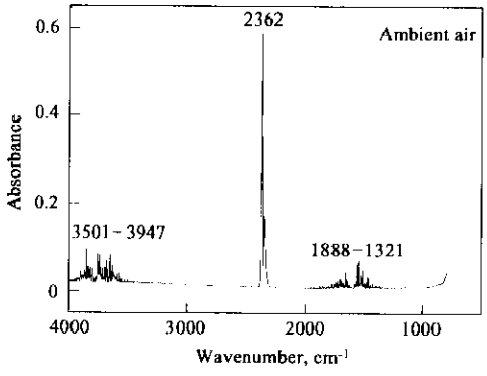

Fig.1 Fourier transformation infrared spectrometer (FTIR) spectrum of ambient air

Fig.2 shows the typical infrared spectrum of toluene/CH_3ONO/NO/air mixture before irradiated by the black lamps. A broad peak at 3077, 3038, 2937, 2883, 2361, 1282, 1113, 1025, 845, 1997—1336 and 3481—3897 cm^{-1} are present. The absorption peaks centered at 2937 and 2883 cm^{-1} are due to aliphatic C—H and that at 3077—3038 cm^{-1} is due to aromatic C—H asymmetrical stretching vibration. They might come from methyl nitrate, toluene and minor products such as 2-hydroxybenzaldehyde. N—O stretch vibration from methyl nitrate, which absorb strongly between 1680—1610 cm^{-1}, is not identified in the studied spectra, perhaps masked by the intensive vibration absorption of water. FTIR vibrational mode due to aromatic ethers is identified around 1025 cm^{-1} (Wang, 1984). Another visible strong peak observed at 1113 cm^{-1} is assigned to the symmetrical vibration of C—O, which comes from tertiary alcohol that was connected to α-unsaturated bond (Wang, 1984). Due to the conjugate effect, the C—O absorption shows a shift from 1150 to 1113 cm^{-1}. The stretching frequencies covering 1997—1336 cm^{-1} and 3481—3897 cm^{-1} are assigned to the water stretching absorptions. From the discussion mentioned above, Fig.2 depicts the infrared spectrum of reactant and minor products. It seems that low concentration of products could also be generated from the dark

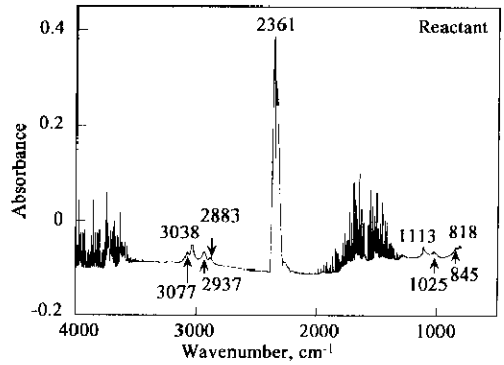

Fig.2 Fourier transformation infrared spectrometer (FTIR) spectrum of toluene/CH_3ONO/NO/Air mixture

reaction of toluene.

Fig.3 shows the infrared spectrum of products from toluene-photooxidation reaction irradiated for one hour. Compared to Fig.2, there exists a strong absorption band around 1674, 1660 and 1635 cm^{-1}, and other absorption peaks also become more intensive, which implies a higher concentration of products. The absorption at 1674 and 1660 cm^{-1} is attributed to the C=O stretching frequency. Because of the conjugate effect of C=C bond, the absorption of C=O shifts from 1715 cm^{-1} to 1674 cm^{-1}. The peak at 1635 cm^{-1} is assigned to stretching vibration of C=C that is connected to carbonyl groups. According to the results of aerosol time of flight mass spectrometer (ATOFMS) measurement (Wang *et al.*, 2006), these absorption peaks might come from 1,4-benzoquinone or 1,2-benzoquinone and other ring-opening products such as 1,4-dioxo-2-butene. While the peak around 1300 cm^{-1} is due to the aromatic C—O groups, and affected by the bending vibration and stretching vibration of C—C bond, its absorption intensity is weaker than that at 1674 cm^{-1}. This functional group might come from aromatic aldyhydes, ketones and carboxylic acids (Wang, 1984). A lower absorption band at 1282 cm^{-1} is assigned to the asymmetrical stretching of aromatic C—O groups. This is in good agreement with what has been reported in the literature regarding the aerosol-phase composition (Jang and Kamens, 2001). The C—O stretching of tertiary alcohol is still shown at 1117 cm^{-1}. It might come from the ring-opening products such as 2-hydroxy-2-methyl-1, 3-propandial (Jang and Kamens, 2001). The absorption at 1020 cm^{-1} is still attributed to aromatic ether. The strong vibrational mode in the range of 850—820 cm^{-1} is assigned to aromatic ring group. A weak absorption at 3218 and 3323 cm^{-1} is due to the O—H stretching vibration of an alcohol or carboxylic acid function group, suggesting a relative lower concentration of O—H in the gas-phase products. The broad absorption bands in the range of 2860—3070 cm^{-1} peaked at 2956 cm^{-1} and 3029 cm^{-1} are assigned to the asymmetrical

stretching vibration of C—H in the aliphatic and aromatic compounds, respectively.

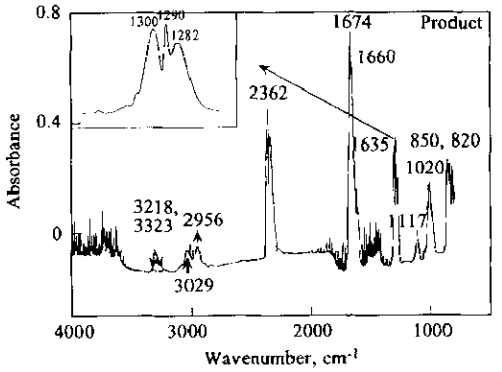

Fig.3 FTIR spectrum of the products from toluene/CH_3ONO/NO mixture irradiated by two black lamps for 1 h

Fig.4 is the background-subtracted FTIR spectra, which is obtained from the difference between the absorption spectrum recorded before and after the mixture of toluene/CH_3ONO/NO/air was irradiated. As shown in Fig.4, two additional absorption peaks masked by the intensive absorption of water, are newly detected, at 1444 and 1514 cm^{-1}. The peak around 1444 cm^{-1} is assigned to C—H vibration of $-CH_2$ groups which is connected to C=C chemical bond. The very weak absorbption at 1514 cm^{-1} is perhaps due to the presence of N—O asymmetrical vibration of nitroaromatic compounds.

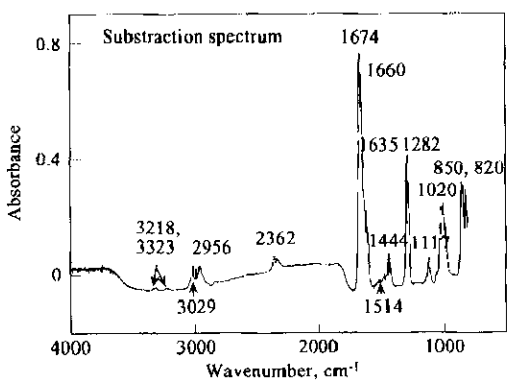

Fig. 4 FTIR subtraction spectra of toluene photoreaction products

2.2 Comparison with FTIR analysis of particles

Fig.5 represents the characteristic FTIR spectrum for secondary aerosols from toluene photooxidation reaction impacted on the ungreased ZnSe FTIR window (Jang and Kamens, 2001). We could find the intensive absorption peak of hydroxyl groups, carbonxylic acid groups, nitroaromatic groups and organonitrate groups. Of these groups, the absorption peak at 1725 cm^{-1} is due to the carbonxyl stretching of carbonxylic acid, ketones and aldehydes. These results are different in part from those of FTIR in the gas-phase products: Organonitrates in the aerosol-phase, formed in the course of most hydrocarbon photooxidation reaction (Jang and Kamens, 2001; Dekermenjian *et al.*, 1999a, b), are not found in the gas-phase products. The strong OH stretching around 3300—3400 cm^{-1} suggests a relative high concentration of alcohol and carboxylic acid compounds in the aerosol-phase products. The differences between the gas and aerosol phase FTIR absorbance perhaps are due to the differences of compounds existing both the gas and aerosol phase products. According to the gas/particle partitioning theory (Odum *et al.*, 1996; Odum *et al.*, 1997a, b), the aerosol-phase products are mainly composed of semivolative and nonvolatile compounds and gas-phase products are semivolative and volatile compounds. By the way, the same absorption peak around 1282 cm^{-1} appears in FTIR of both the gas-phase and aerosol-phase products indicating that both of them containing the same C—O groups. Table 1 lists these important functional groups both in the gas and aerosol-phase products.

In order to verify the presence of function groups in the aerosol phase, we have used aerosol time of flight mass spectrometer to measure the molecule composition and size of individual SOA particle

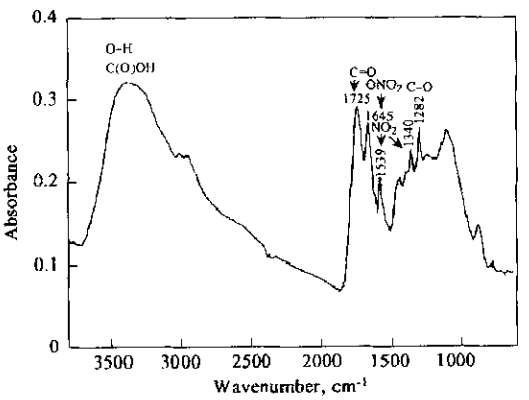

Fig.5 FTIR spectrum for secondary aerosols impacted on the ungreased FTIR window (Jang and Kamens, 2001)

Table 1 Assignment of functional groups in the products

Functionality	Absorbance band, cm^{-1}	
	Gas phase (this work)	Particle phase (Jang and Kamens, 2001)
Aliphatic C—H	2956	2800—3000
Aromatic C—H	3029	3000—3100
C=O (C=O—C—)	1674	1640—1780
C=C	1635	/
Aromatic C=O	1300	/
Aromatic C—O	1282, 1020	1282
C—O	1117	/
O—H (alcohols)	3218	3100—3500
O—H (COOH)	3323	2500—3300
C—H ($-CH_2$ C=C)	1444	/
C—H (aromatic ring)	850—820	/
O—N	1514	/
R—ONO_2	/	1645
—NO_2	/	1559, 1342

simultaneously in the laboratory (Wang *et al.*, 2006). According to the experimental results, each aerosol particle corresponds to a piece of mass spectrum, and the diameter and chemical composition of each particle might be different from each other. Fig. 6 shows the mass spectra of one individual particle with aerodynamic diameter of 1.844 μm. From the composition of a number of individual particles, we get the composition of SOA particle statistically. Enclosed here are some typical compounds, such as: 1,4-dioxo-2-butene ($C_4H_4O_2$, m/z=84); 2-hydroxy-1,3-propandial or 2-oxopropanic acid ($C_3H_4O_3$, m/z=88); ethane diacid ($C_2H_2O_4$, m/z=90); benzaldehyde (C_7H_6O, m/z=106); *n*-butane diacid ($C_4H_6O_4$, m/z=118); methylphenylketone or 2-methyl-benzadehyde (*m*-, *p*-isomers; C_8H_8O, m/z=120); Peroxyacyl nitrates (PAN, $C_2H_3O_5N$, m/z=121); benzoic acid, 2-methyl-benzoquinone or 2-hydroxy-benzaldehyde (*m*-, *p*-isomers; $C_7H_6O_2$, m/z=122); nitrobenzene ($C_6H_5NO_2$, m/z=123); 2,3-dihydroxy-4-oxobutanic acid ($C_4H_6O_5$, m/z=134). These compounds may belong to aliphatic and aromatic compounds with special functional groups of aromatic C—H bonds, aliphatic C—H bonds, carbonyl groups (C=O), hydroxyl groups (R—OH), C=C bonds, nitroaromatic groups ($R—NO_2$) and organonitrate groups ($R—ONO_2$). These results are in good agreement with those obtained by FTIR in the aerosol phase.

It should be pointed out that ATOFMS and FTIR spectroscopy of gas phase used to analyze the toluene-photooxidation products were generated under the same experimental conditions.

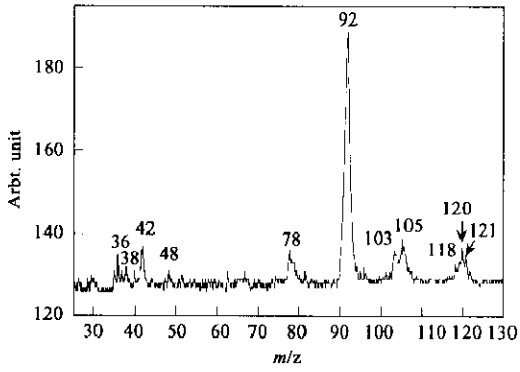

Fig.6 Positive ion mass spectra of individual particle (aerodynamic diameter is 1.844 μm)

2.3 Possible reaction pathway for some products

In Fig.3, the intensive absorption of C=O group and C—O chemical bond indicated a higher level of compounds bearing these functional groups. Here we will account for the possible reaction pathways of these compounds. Of the aromatic hydrocarbons studied, oxidation reaction of toluene proceeds primarily with hydroxyl radical. The toluene-OH reaction results in 10% H-atom abstraction from the methyl group and 90% OH addition to the aromatic ring (Forstner *et al.*, 1997):

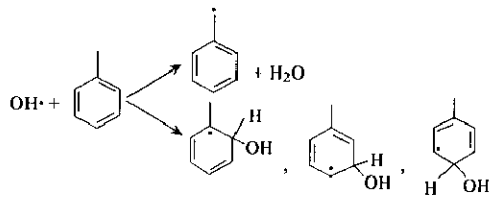

(Pathway 1)

In high concentration of O_2 and NO, the hydrogen abstraction pathway will result in the formation of aromatic aldehydes. Since H atom abstraction is a minor pathway, the functional groups generated by pathway 2 are also present at relative low concentration in the gas phase.

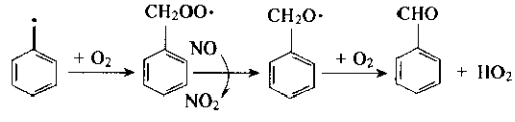

(Pathway 2)

The major route for the reaction of toluene is the addition of hydroxyl radical to the aromatic ring, forming an OH-toluene adduct. The OH radical can add to toluene in the ortho, meta and para positons, with the ortho position energetically favored (Forstner *et al.*, 1997). The adduct will reaction with O_2 and NO, undergoing a series of subsequent reactions, forming the intermediate of hydroxyl-toluene and peroxy radical, finally resulting in the formation of ring-retaining products such as 2-hydroxyl-benzaldehyde, 2-hydroxyl-benzonic acid, 2-methyl-benzoquinone and the isomers. These compounds perhaps contribute greatly to the absorption peaked at 1674 and 1300 cm^{-1}. The product of 2-methyl-benzoquinone can be attacked by OH again, react with O_2, leading to forming 3-methyl-3-hydroxyl-2,4, 5-trioxo-valeric acid, the C—O chemical bond contained in these compounds may contribute to the absorption at 1117 cm^{-1}. The details of this mechanism are outlined in pathway 3.

One route of the reaction of adduct with O_2 can yield an aromatic alcohol which subsequently form unsaturated oxygenates. Another route of the same reaction can directly form unsaturated oxygenates, without the hydroxyl aromatic as an intermediate. The oxygenates cleave to form unsaturated dicarbonyls, as shown in pathway 4. If the hydroxyl radical reacts with the unsaturated dicarbonyl by addition of the carbon double bond, as shown in pathway 5, it will form hydroxy-tricarbonyl compound (a). The hydroxy-tricarbonyl can transform into an unsaturated dihydroxy-dicarbonyl compound (b). This compound can be oxided to form polyketone. The strong

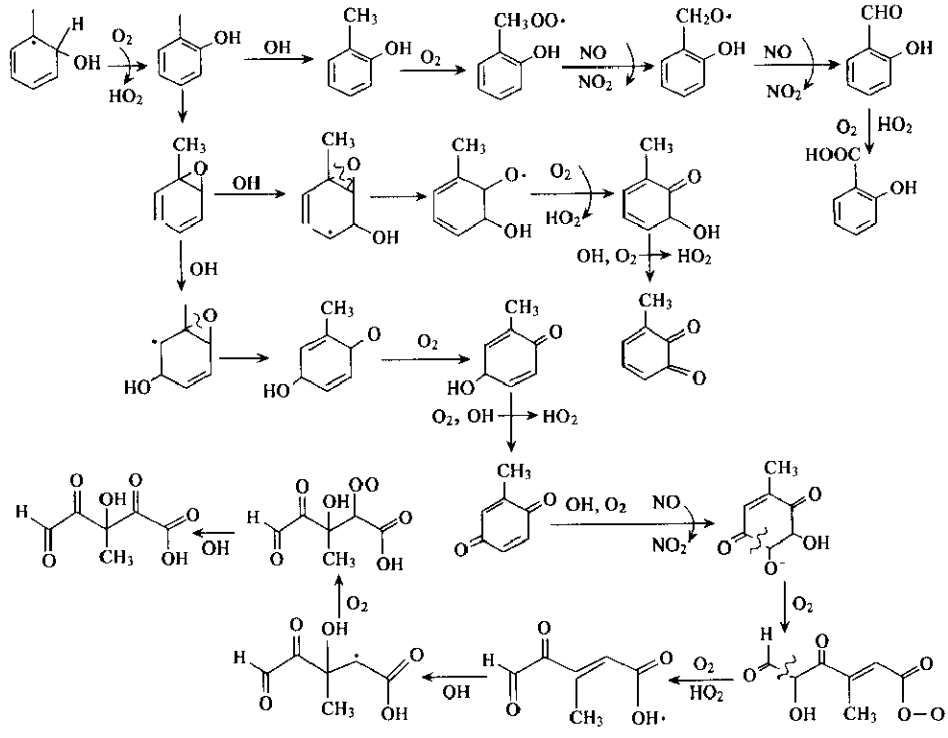

(Pathway 3)

absorption of C=O groups in Fig.5 possibly come from these compounds.

As noted above, there list only the possible reaction pathway of some products. The functional groups contained in these products are clearly identified in the analysis results of ATOFMS and FTIR.

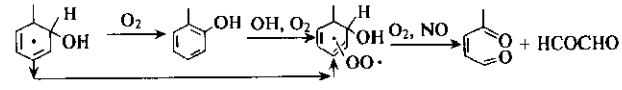

(Pathway 4)

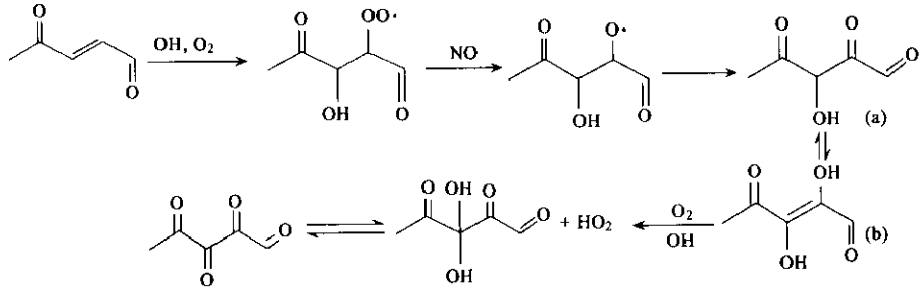

(Pathway 5)

3 Conclusions

OH-initiated photooxidation reaction of toluene was carried out in a smog chamber. The gas-phase products from toluene photooxidation and its subsequent reaction were analyzed directly by FTIR. The results were compared with those in the aerosol-phase products analyzed by ATOFMS and FTIR. Analysis of infrared spectra in gas phase indicated that the molar loadings of carbonyl groups connected to unsaturated chemical bond were significant. ATOFMS mass spectrum and FTIR spectrum showed the presence of ketones, aldehydes, carbonxylic acid and organonitrates in the aerosol-phase products. These results indicated that information of the functional groups contained in the gas phase products was different in part from that in the aerosol phase. These perhaps will contribute to obtain information on the gas/particle phase distribution of the products.

References:

Atkinson R, Carter W P L, Winer A M *et al.*, 1981. An experimental protocol for the determination of OH radical rate constants with organics using methyl nitrite photolysis as an OH· radical source [J]. J Air Pollution Control Association, 31: 1090—1092.

Bowman F M, Odum J R, Seinfeld J H *et al.*, 1997. Mathematical model for gas-particle partitioning of secondary organic aerosols [J]. Atmos Environ, 31: 3921—3931.

Dekermenjian M, Allen D T, Atkinson R *et al.*, 1999a. FTIR analysis of aerosol formed in the photooxidation of naphthalene [J]. Aerosol Sci Technol, 30: 273—279.

Dekermenjian M, Allen D T, Atkinson R *et al.*, 1999b. FTIR analysis of aerosol formed in the ozone oxidation of sesquiterpenes [J]. Aerosol Sci Technol, 30: 349—363.

Etzkorn T, Klotz B, Sorensen S *et al.*, 1999. Gas-phase absorbtion cross section of 24 monocyclic aromatic hydrocarbons in the UV and IR spectral ranges [J]. Atmos Environ, 33: 525—540.

Forstner H J L, Flagan R C, Seinfeld J H, 1997. Secondary organic aerosol from the photooxidation of aromatic hydrocarbons: molecular composition [J]. Environ Sci Technol, 31: 1345—1350.

Frazey P, Rao X, Spaulding R *et al.*, 1999. The power of pentafluorobenzyl alcohol chemical ionization/ion trap mass spectroscopy to identify pentafluorobenzyl derivatives of oxygenated polar organics [J]. Int J Mass Spectroscopy, 191: 343—357.

Hao L Q, Wang Z Y, Huang M Q *et al.*, 2005. Size distribution of the secondary organic aerosol particles from the photooxidation of toluene[J]. J Environ Sci, 17(6): 912—916.

Jacob D J, 2000. Heterogeneous chemistry and tropospheric ozone[J], Atmos Environ, 34: 2131— 2159.

Jang M, Kamens R M, 2001. Characterization of secondary aerosol from the photooxidation of toluene in the presence of NOx and 1-proprene[J]. Environ Sci Technol, 35: 3626—3639.

Jang M S, Czoschke N M, Lee S *et al.*, 2002. Heterogeneous atmospheric aerosol production by acid-catalyzed particle-phase reactions[J]. Science, 298: 814—817.

Kalberer M, Paulsen D, Sax M *et al.*, 2004. Identification of polymers as major components of atmospheric organic aerosols [J]. Science, 303: 1659—1622.

Kleindienst E, Conver T S, Mclver C D *et al.*, 2004. Determination of secondary organic aerosol products from the photoxidation of toluene and their implications in ambient $PM_{2.5}$ [J]. J Atmos Chem, 47: 79—100.

Klotz B, Volkamer R, Hurley M D *et al.*, 2002. OH-initiated oxidation of benzene Part II. Influence of elevated NOx concentration[J]. Phys Chem Chem Phys, 4: 4399—4411.

Klotz B, Barnes I, Becker K H *et al.*, 1997. Atmospheric chemistry of benzene oxide oxepin [J]. J Chem Soc Faraday Trans, 93(8): 1507—1516.

Odum J R, Hoffmann T, Bowman F *et al.*, 1996. Gas/particle partitioning and secondary organic aerosol yields[J]. Environ Sci Technol, 30: 2580—2585.

Odum J R, Jungkamp T P W, Griffin R J *et al.*, 1997a. Aromatic reformulated gasoline, and atmospheric organic aerosol formation[J]. Environ Sci Technol, 31: 1890—1897.

Odum J R, Jungkamp T P W, Griffin R J *et al.*, 1997b. The atmospheric aerosol-forming potential of whole gasoline vapor [J]. Science, 276: 96—99.

Stroud C A, Makar P A, Michelangeli D V *et al.*, 2004. Simulating organic aerosol formation during the photooxidation of toluene/NOx mixtures: Comparing the equilibrium and kinetic assumption[J]. Environ Sci Technol, 38: 1471—1479.

Suh I, Zhang D, Zhang R Y *et al.*, 2002. Theoretical study of OH addition reaction to toluene [J]. Chem Phys Lett, 363: 454—462.

Uc V H, Garcia-Cruz I, Hernandez-Laguna A *et al.*, 2000. New channels in the reaction mechanisms of the atmospheric oxidation of toluene [J]. J Phys Chem A, 104: 7847—7855.

Volkamer R, Klotz B, Barnes I *et al.*, 2002. OH-initiated oxidation of benzene Part I. Phenol formation under atmospheric conditions [J]. Phys Chem Chem Phys, 4: 1598—1610.

Wang X M, 1984. Analysis using infrared spectrometer [M]. Beijing: Scientific Press. 37.

Wang Z Y, Hao L Q, Zhang W J, 2005. Chemical process on the formation of secondary organic aerosols [J]. Progress in Chemistry, 17(4): 732—736.

Wang Z Y, Hao L Q, Zhou L Z *et al.*, 2006. Real-Time detection of individual secondary organic aerosol particle from photooxidation of toluene using aerosol time of flight mass spectrometer[J]. Sci in China, Ser B, 49(3): 267—272.

Weingartner E, Frankevich V, Zenobi R *et al.*, 2004. Identification of polymers as major components of atmospheric organic aerosols [J]. Science, 303: 1659—1662.

(Received for review November 21, 2005. Accepted January 23, 2006)